

## The Ability of *Rhizopus stolonifer* MR11 to Biosynthesize Silver Nanoparticles in Response to Various Culture Media Components and Optimization of Process Parameters Required at Each Stage of Biosynthesis

Khaled Khleifat<sup>1</sup>, Moath Alqaraleh<sup>2</sup>, Muhamad Al-limoun<sup>3</sup>, Ibrahim Alfarrayeh<sup>3\*</sup>, Rasha Khatib<sup>3</sup>, Haitham Qaralleh<sup>4</sup>, Ahmad Alsarayreh<sup>3</sup>, Yaseen Al Qaisi<sup>3</sup>, Maha Abu Hajleh<sup>5</sup>

<sup>1</sup> Faculty of Allied Medical Sciences, Al-Ahliyya Amman University, Amman, Jordan

<sup>2</sup> Pharmacological and Diagnostic Research Center (PDRC), Faculty of Pharmacy, Al-Ahliyya Amman University, Amman, 19328, Jordan

<sup>3</sup> Department of Biological Sciences, Faculty of Science, Mutah University, Al-Karak, 61710, Jordan

<sup>4</sup> Department of Medical Analysis, Faculty of Science, Mutah University, Al-Karak, 61710, Jordan

<sup>5</sup> Department of Cosmetic Science, Pharmacological and Diagnostic Research Center (PDRC), Faculty of Allied Medical Sciences, Al-Ahliyya Amman University, Amman, Jordan

\* Corresponding author's e-mail: alfarrayeh@gmail.com

### ABSTRACT

One of the most important roles for nanotechnology concerns is the development of optimizable experimental protocols for nanomaterials synthesis. The formation of silver nanoparticles (AgNPs) was supported by *Rhizopus stolonifer* MR11, which was isolated from olive oil mill soil samples. The ability of *R. stolonifer* MR11 to biosynthesize silver nanoparticles in response to various components of different culture media was tested. Furthermore, the conditions under which the reducing biomass filtrate was obtained, as well as the conditions of the bio-reduction reaction of AgNO<sub>3</sub> into AgNPs, were investigated. The fungal biomass filtrate of the strain *Rhizopus stolonifer* MR11 was capable of converting silver nitrate into AgNPs, as evidenced by the color change of the fungal filtrates. UV-Vis spectrophotometer, TEM, Zeta potential, Zeta sizer, FT-IR, and XRD analyses were used to characterize the AgNPs. TEM analysis revealed that the silver nanoparticles were 1–35 nm in size. *R. stolonifer* MR11 produced the maximum AgNPs when grown for 18 hours at 36 °C in media with starch and yeast extract as the sole carbon and nitrogen sources, respectively. The reducing biomass filtrate was obtained by incubating 5 g mycelial biomass in deionized water with a pH of 6 for 48 hours at 30 °C. The optimal reduction conditions of the biosynthesis reaction were determined by adding 1.0 mM AgNO<sub>3</sub> to a pH 5 buffered mycelial filtrate and incubating it for 72 hours at 33 °C. The current study's findings highlighted the importance of process parameters at each stage for optimal AgNPs biosynthesis.

**Keywords:** nanotechnology, silver nanoparticles, *Rhizopus stolonifer* MR11, optimization, characterization.

### INTRODUCTION

Nanoscience is primarily concerned with the structural, physical, and chemical aspects of nanoscale objects. On the other hand, nanotechnology is seen as the commercial, industrial, environmental, and medicinal application of the acquired

fundamental knowledge of nano-objects (Satalkar et al., 2016). Nanoscience and nanotechnology are both new and active sectors of science that include multi-interdisciplinary sciences (Sergeev and Shabatina, 2008).

All nanoscale substances, regardless of their nature and structure, are referred to as

nano-objects, where the prefix ‘nano’ means one-millionth of millimeter size. The word objects can be specifically replaced by any other word that describes the nature of these objects (Ingole et al., 2010) which can be particles, fibers, or plates (Calderón-Jiménez et al., 2017). The outcomes of basic knowledge about nano-sized objects altered the viewpoints of the industrial world, whose goods today incorporate nanoscale building blocks and raw materials (Ingole et al., 2010).

However, nanoparticles (NPs) are three-dimensional geometrical forms made up of groups of atoms, with at least one of their three exterior dimensions ranging from 1 to 100 nm (Calderón-Jiménez et al., 2017; Williams, 2008). Compared to their larger counterparts, they show exceptional and different size-related Physico-chemical properties (Colvin et al., 1994; Xu et al., 2006). Because of their nano size and large surface area, metal nanoparticles could have exclusive and novel physical and chemical properties in comparison to their macroscale counterparts (Gentile et al., 2016). Among metal nanoparticles silver nanoparticles (AgNPs) successfully found their way into many products such as plastics, textiles, and soaps (Dallas et al., 2011; Fabrega et al., 2011; García-Barrasa et al., 2011). Moreover, they could be very interesting and popular antimicrobial agents with broad-spectrum activity against a variety of microorganisms.

Three main approaches which are routinely used for the synthesis of metal nanoparticles include the chemical, physical and biological methods. biological approaches are considered as eco-friendly, cheap, and safe since they do not require the utilization of toxic substances and are free of resulting hazardous byproducts. They include several intracellular and extracellular biological methods that use bacteria, fungi, plants, or their extracts and are known collectively as green nanotechnology (Klaus et al., 1999). The current study aimed to evaluate the influence

of culture conditions of *R. stolonifer* MR11 on the ability of the fungal filtrate to biosynthesize AgNPs, optimize the reduction potential of *R. stolonifer* MR11 biomass filtrate used in AgNPs biosynthesis, determine the best reaction conditions for AgNPs biosynthesis, and characterize the biosynthesized AgNPs.

## MATERIALS AND METHODS

### Fungal strain

The fungal isolate utilized in this study was discovered in the soil of an olive oil mill in Jordan's southern of the Al-Karak area. ITS sequencing (MACROGEN, Korea) and sequence matching within the NCBI database were used to identify this isolate as *Rhizopus stolonifer* MR11, and the accession number obtained was MN259123.

### Biosynthesis of AgNPs

Filtering the aqueous suspension containing the fungal biomass using Whatman No. 1 filter paper yielded the fungal filtrate. AgNO<sub>3</sub> was added to the fungus filtrate at a concentration of 1 mM in 100 mL and incubated in the dark at 33 °C and 150 rpm for 24 hours to generate biosynthesized AgNPs. The synthesis of AgNPs was tracked during the incubation process using spectrophotometric analysis, UV/VIS (280-800 nm). At the same time, the AgNO<sub>3</sub>-free flask was incubated under identical conditions as the control flask (Jaidev and Narasimha, 2010).

### Effects of culture conditions of *R. stolonifer* MR11 on AgNPs biosynthesis

The study also investigated the effect of different fungal cultivation conditions on fungal biomass, such as the variation in the chemical

**Table 1.** Chemical composition of the tested media

Media	Chemical composition % (w/v)
M1	1.0% (w/v) glucose, 0.3% (w/v) yeast extract, 0.3% (w/v) malt extract, 0.5 % (w/v) peptone and 0.5% (w/v) NaCl
M2	1.0% (w/v) glucose, 1.0% (w/v) yeast extract and 0.5% (w/v) NaCl
M3	0.2% (w/v) glucose, 0.2% (w/v) fructose, 0.2% (w/v) mannose, 0.2% (w/v) mannitol, 0.2% (w/v) sorbitol, 0.1 % of potassium nitrate, 0.9% yeast extract and 0.5 % (w/v) NaCl
M4	1.0% (w/v) sucrose, 1.0% (w/v) yeast extract and 0.5% (w/v) NaCl
M5	1.0% (w/v) starch, 1.0% (w/v) yeast extract and 0.5% (w/v) NaCl

composition of growth media (Table 1), pH levels of 3, 4, 5, 6, and 7, and the temperature of the growth incubation at 30, 33, 36, and 39 °C, as well as the length of the incubation period, which involved 18, 24, 36, 48, and 72 hours. As detailed in section 2.2, the biomass filtration procedure utilized to create AgNPs was carried out and monitored using assay spectroscopy.

### Optimization of the reduction potential of *R. stolonifer* MR11 biomass filtrate

In order to achieve the best-operating conditions to obtain the highest reduction potential of the fungal biomass filtrate, the effects of the time course of biomass-deionized water mixture duration, utilized biomass amount, pH of the buffered deionized water, and incubation temperature were studied. The collected biomass used in this part of the study was obtained by growing the fungus in the growth medium number 5 under the optimum conditions as obtained from the previous experiments. The initial conditions to obtain the biomass filtrate used in AgNPs formation were 10 g wet weight biomass, 33 °C, pH 7.0 buffered deionized water, 150 rpm agitation speed for 25 hrs. The best incubation duration of the deionized water-fungal biomass mixture was obtained by collecting the filtrate after 24, 48, 72, and 96 hrs. To evaluate the effects of the utilized fungal biomass amounts on the reduction potential of the filtrate, different quantities of biomass (2.5, 5.0, 10, and 15 grams) were submerged in buffered deionized water and the generated filtrate was utilized for AgNPs formation. In the next phase, different pH values of the deionized water were employed (pH 4, 5, 6, 7, and 8) by using 25 mM buffer systems (citrate solution for pH 4, 5, and 6, phosphate solution for pH 7, and Tris-HCl buffer, pH 8). As described in section 2.2, the effect of varying the incubation temperature (30, 33, and 36 °C) on the reduction potential of the biomass filtrate to make AgNPs was investigated using scanning spectrophotometric analysis.

### Optimization of AgNPs biosynthesis reaction

Similar to the optimization of the reduction potential of *R. stolonifer* MR11 biomass filtrate in the previous section, for the optimizing of AgNPs biosynthesis reaction by mycelia-free fungal

filtrate, four essential criteria were applied. These variables include the reaction pH (4.0, 5.0, 6.0, 7.0 and 8.0), AgNO<sub>3</sub> concentration (0.25, 0.5, 0.75 and 1.0 mM), time course of the biosynthesis reaction (12, 18, 24, 36, 48, 60, 72 and 80 hrs) and reaction temperatures (30, 33 and 36 °C). Parameters were optimized by employing a single parameter at a time and then applying the improved parameter to the next parameter. The production of AgNPs was studied utilizing spectrophotometric scanning analysis.

### Characterization of AgNPs

The synthesis of AgNPs nanoparticles was quantitatively tracked by UV-scanning spectrophotometry (Shimadzu, Japan), which is directly proportional to the strength of the brown color generated. Centrifugation at 15,000 rpm for 20 minutes to separate the biosynthesized silver nanoparticles from the reaction mixture was carried out (MIKRO 200 R, Hettich, Germany), and the precipitation technique was repeated after re-immersion of the obtained precipitated AgNPs in deionized water, and so on. After that, the AgNPs pellets were dried in a vacuum oven (VWR 1410 Vacuum Oven, USA). AgNP shape, size, and distribution were studied using TEM imaging. XRD-7000 and MAXima-X were used to define the structure and shape of a crystal for biosynthesized AgNPs (SHIMADZU, Japan). Using a Bruker Alpha FTIR spectrometer, functional groups such as proteins responsible for AgNP stability were identified (Bruker Optics GmbH, Ettlingen, Germany).

### Z-potential and Zetasizer distribution by intensity

The particle size and zeta potential of AgNPs were determined using the Zetasizer Nano-ZS90 (Malvern Instruments, UK). The analysis was performed at a temperature of 25 °C and a scattering angle of 90 using various intensities of samples diluted with non-ionized distilled water.

## RESULTS AND DISCUSSION

In this experiment, the fungal isolate *R. stolonifer* MR11 was cultured in a growth suspension after being isolated from contaminated soil and identified using ITS sequence alignment

results. Subsequently, reductant fungal filtrate was prepared from the collected biomass and ultimately used in the reduction of AgNO<sub>3</sub> into AgNPs. Incubation with the fungal filtrate causes the transformation of AgNO<sub>3</sub> to a brown color, indicating the formation of AgNPs. On the other hand, the control flasks remain without changing in color throughout the time of incubation. The surface plasmon resonance (SPR) exemplified by the nanoparticles results in the development of a brown to dark brown color. The obtained peaks of the absorbance of AgNPs solution are usually found to be between 400 and 450 nm and resulted peaks at longer wavelengths represent large nanoparticles (Elamawi et al., 2018). The size and shape of the AgNPs accurately represent the absorbance peak (Jaidev and Narasimha, 2010). The fungal strain used, incubation temperature, reaction medium pH, and the existence of capping agents all influence the capacity of AgNPs synthesis, size, shape, and revealed absorbance peaks (Lee and Jun, 2019).

### **Effects of culture conditions on AgNPs formation**

The effect of cultivation conditions such as artificial media, pH, temperature, and growth period length on the emergence of AgNPs by *R. stolonifer* MR11 biomass filtrate was probed.

#### *Effects of the chemical composition of the growth media on AgNPs formation*

Five culture media with different chemical compositions were used to grow *R. stolonifer* MR11 in order to investigate the effects of changes in the chemical constituents of growth media on the potential of *R. stolonifer* MR11 biomass filtrate to synthesize AgNPs. The results of the ultraviolet-visible spectrophotometric analysis of the AgNPs produced by *R. stolonifer* MR11 using the biomass filtrate obtained from the tested media are shown in Figure 1A. The color of the reaction solution of AgNO<sub>3</sub> using the fungal biomass filtrate obtained by growing the fungus in medium number 5 (containing polysaccharide carbon source) was slightly altered from pale yellow to light brown indicating the low formation of AgNPs. Meanwhile, no detectable changes in the color of the controls and AgNPs biosynthesis reaction media using

the biomass filtrates of other media (containing simple sugars as carbon sources) were observed. This result indicates that nanoparticle synthesis was generally relieved of the repression exacerbated by other simple carbon sources tested in other media. However, the amount of AgNPs biosynthesis was expressed incoherently as an increment in absorbance or the appearance of a clear peak at wavelengths near 400 nm, because this wavelength range was a characteristic peak for AgNPs synthesis. As a result, the color change was directly related to the quantity of AgNPs formed (Bhainsa and D'souza, 2006; Padalia et al., 2015).

#### *Effect of pH value of the growth media on AgNPs formation*

The results of the effect of the pH alterations in the best culture medium selected from the previous experiment (medium number 5) are shown in Figure 1B. The biomass filtrate obtained by growing the fungal strain with an initial pH of 5 contributed to the preferred creation of AgNPs. The absorbance curve of the prepared AgNPs by the filtrate of the biomass grown in a medium with pH 5 (Figure 1B) clearly showed an absorbance peak at 426 nm. However, other biomass filtrates resulting from the mycelial biomass collected from the culture media with pH values of 3, 4, and 6 also supported the formation of AgNPs but to less extent. Meanwhile, the reductant filtrate obtained from the mycelial biomass grown in the culture medium with pH 7 did not show any clear AgNPs formation peak.

#### *Effects of incubation temperature on AgNPs formation*

Figure 1C demonstrates the results of the effect of incubation temperature on the utilized biomass filtrate AgNPs biosynthesis ability. The best incubation temperature that showed the best reductant filtrate resulted in the highest AgNPs formation was 33 °C with an absorbance peak at 427 nm. However, higher or lower incubation temperatures resulted in mycelial biomass with less AgNPs biosynthesis ability.

#### *Effects of culture time profile on AgNPs formation*

The impact of the culture time profile on the ability of *R. stolonifer* MR11 biomass filtrate in the formation of AgNPs was also investigated and the results are presented in Figure 1D. The

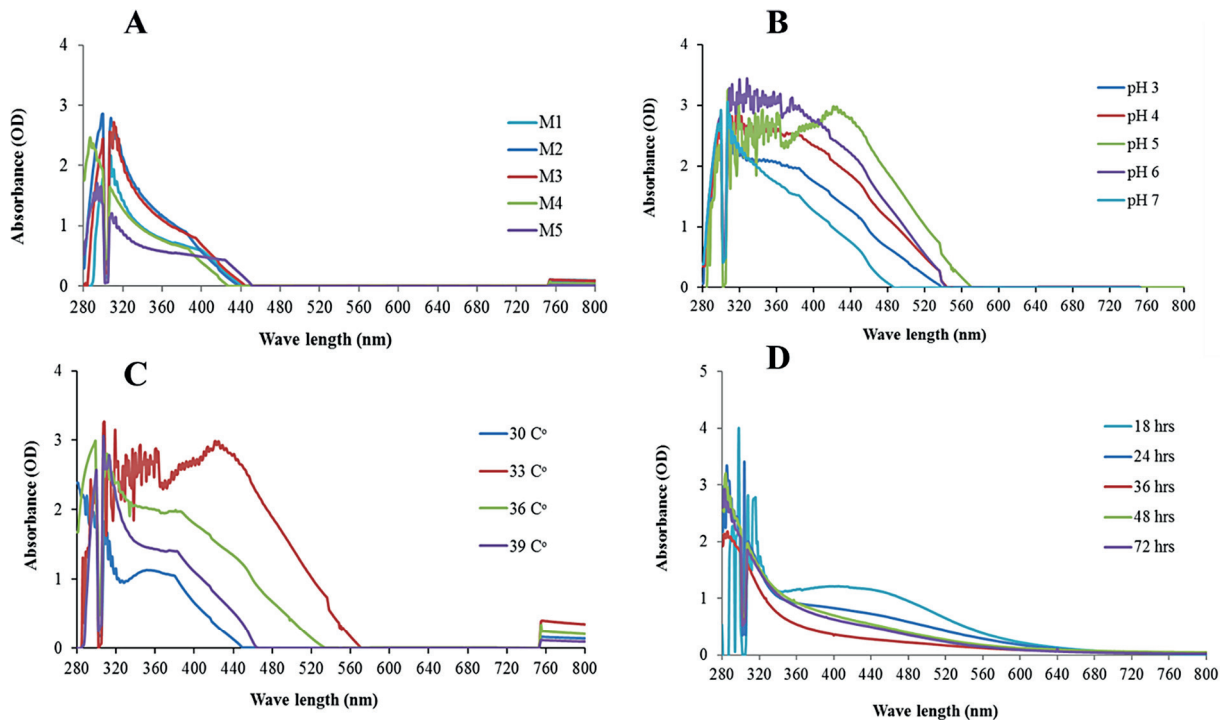


**Figure 1.** A) Effects of culture media composition on AgNPs formation; B) Effects of culture media pH on AgNPs formation; C) Effects of culture incubation temperature on AgNPs formation; D) Effects of culture time profile on AgNPs formation

highest intensity of the AgNPs solution brownish color was observed when the filtrate was prepared from the mycelial biomass that collected after 18 hrs of growth. Growing *R. stolonifer* MR11 for longer periods of time resulted in biomass with lower reduction ability as demonstrated by the color intensity of AgNPs solution and spectrophotometric scan.

Generally, the mechanism of nanoparticles biosynthesis is not fully understood. More specifically, the mechanism by which fungi biosynthesize AgNPs is not yet explained but its most probably mediated by an enzymatic system of reductases reducing the  $\text{Ag}^+$  of  $\text{AgNO}_3$  into  $\text{Ag}^0$  elementary metal that clusters into nanoscale particles (Guilger-Casagrande and Lima, 2019).

Two possible mechanisms for the formation of AgNPs by *Fusarium oxysporum* and *Bacillus licheniformis* were reported. The first is through NADH-dependent nitrate reductase (Mukherjee et al., 2002), and the second is by shuttle quinone process (Basavaraja et al., 2008; Durán et al., 2005; Jaidev and Narasimha, 2010; Kalimuthu et al., 2008). Like any other biomolecules, the biosynthesis of such reductases is influenced by the growth conditions under which the microorganism is grown. Therefore, the variations in the culture conditions will be

reflected as variations in the amounts of reductases and other reductant biomolecules released into the filtrate that ultimately affects the biosynthesis of AgNPs.

### Biomass filtrate reduction potential optimization

#### Optimization of the incubation period

In this experiment, the best incubation period for the mycelial biomass with the deionized water to create reducing filtrate with maximum reduction ability was evaluated. The collected fungal filtrate was taken at regular intervals of 24, 48, 72, and 96 hours. The results in Figure 2A showed that the rate of synthesis progressively developed in intensity as a function of incubation time peaked at 48 hrs until the incubation time reached 72 hrs, beyond which the rate of AgNPs synthesis declined.

#### Optimization of the cell mass

The influence of different cell masses utilized to create the reducing filtrate was studied by mixing 2.5, 5, 10, and 15 g wet weight mycelial biomass with the deionized water. As shown in Figure 2B, 2.5, 5, and 10 g of cell

mass led to the formation of AgNPs. However, 5 g biomass displayed the highest amount of AgNPs. The present data pointed to an effective role played by optimized cell mass for enhancing the nanoparticles synthesis by the filtrate of *R. stolonifer* MR11 cells. Balakumaran et al. (2015) and Singh et al (2014) both emphasized the importance of biomass concentration in enhancing AgNPs synthesis

#### Optimization of the pH value

A number of pH buffers (4, 5, 6, 7, and 8) were used to investigate the impact of the pH level of the deionized water used to produce the ultimate filtrate being used AgNPs biogenesis. Maximum AgNPs creation capability was observed at the acidic pH of 6 (Figure 2C). Other pH values like 5 and 7 resulted in a lower ability of AgNPs biosynthesis. It was revealed that particle size could be monitored by adjusting physical conditions such as temperature, pH, and AgNO<sub>3</sub> concentration (Gurunathan et al., 2009). Balakumaran et al. (2015) reported the importance of pH as a key factor in nanoparticle formation. In contrast to our results, the formation of AgNPs was favored at alkaline pH using the fungus *Epicoccumnigrum* (Qian et al., 2013).

#### Optimization of the incubation temperature

The fungal biomass was suspended in buffered sterilized deionized water and incubated at diverse temperatures (30, 33, and 36 °C). Based on the AgNPs solution color intensity and absorbance scan, the maximum rate of AgNPs biosynthesis was attained at 30 °C (Figure 2D). Under higher incubation temperatures of 33 and 36 °C, a significant decrease in AgNPs formation was found as shown by the color strength of the nanoparticles solution as well as the spectrophotometric analysis. Elamawi et al. (2018) reported similar results when they incubated five amounts of *T. longibrachiatum* biomasses at temperatures lower or higher than the optimum (28 °C) showing no or lower Ag nanoparticles formation.

### Optimization of AgNPs biosynthesis reaction conditions

#### pH values optimization

In overall, the "reduction capacity" of a metallic reaction is affected by the pH of the solution because it can affect the morphological characteristics of the yield over the creation of certain species, as demonstrated (Sanghi and Verma, 2009). The current study investigated

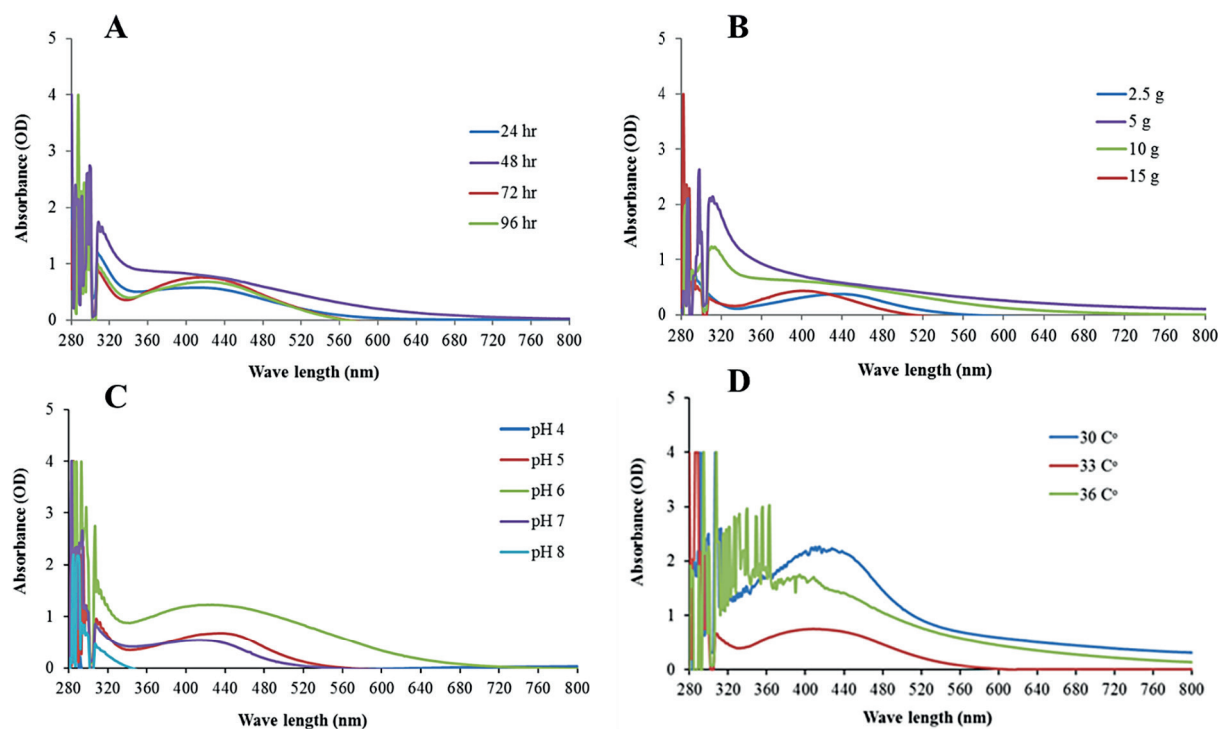


**Figure 2.** Effect of different conditions of biomass-deionized water mixture on the reduction potency of biomass filtrate (A) Incubation term; (B) Cell mass; (C) pH level variation and (D) Incubation temperature

pH-dependent variability in the reaction medium for maximum Synthesis of AgNPs. According to the findings of our study, the utmost biosynthesis of AgNPs was perceived at acidic pH of 5.0, meanwhile higher or lower pH values showed no or lower Ag nanoparticles formation (Figure 3A). It has been reported previously that an increase or decrease in the pH from the optimum can lead to the accumulation or alteration of Ag particles (Gurunathan et al., 2009). In contrast to our results, previous studies stated that the provision of an alkaline ion is essential to boost the reduction reaction of metal ions (Sanghi and Verma, 2009).

#### AgNO<sub>3</sub> concentration optimization

Various amounts of AgNO<sub>3</sub> (0.25, 0.5, 0.75, 1.0, and 1.5 mM) were examined to prove whether AgNO<sub>3</sub> concentration performs an important role in the formulation of nanoparticles. The effect of AgNO<sub>3</sub> concentration on the emergence of AgNPs is depicted in Figure 3B. The rate of synthesis was found to be greatest at 1.0 mM, with lower and higher concentrations having a slower rate of bioreduction. This may be due to enzyme-substrate kinetic saturation (Alfarayeh et al., 2021b; Singh et al., 2013).

#### Reaction time optimization

Figure 3C shows the outcome of the reaction period on the materialization of AgNPs. The highest production of AgNPs was observed after 48 hrs of running the biosynthesis reaction with the maximum recorded at 72 hrs. Lower production of AgNPs was observed at lower reaction times such as 12, 18, 24, and 36 hrs. In contrast to our results, faster formation of AgNPs was achieved using the endophytic fungi *G. mangiferae* with 12 hrs as the best incubation time under optimized reaction conditions (Balakumaran et al., 2015). Similarly, Singh et al. (2014) also reported the maximum formation of AgNPs using *Penicillium* sp. within 24 hrs incubation time.

#### Reaction temperature optimization

The effect of the reaction temperature on the synthesis of nanoparticles was investigated by tracking the bioreductive capacity of the reaction temperature and the results are shown in Figure 3D. The biosynthesis rate of AgNPs increased with increasing temperature up to 33 °C, after which the synthesis of silver nanoparticles decreased. The increased rate of AgNPs synthesis could be attributed to the influence

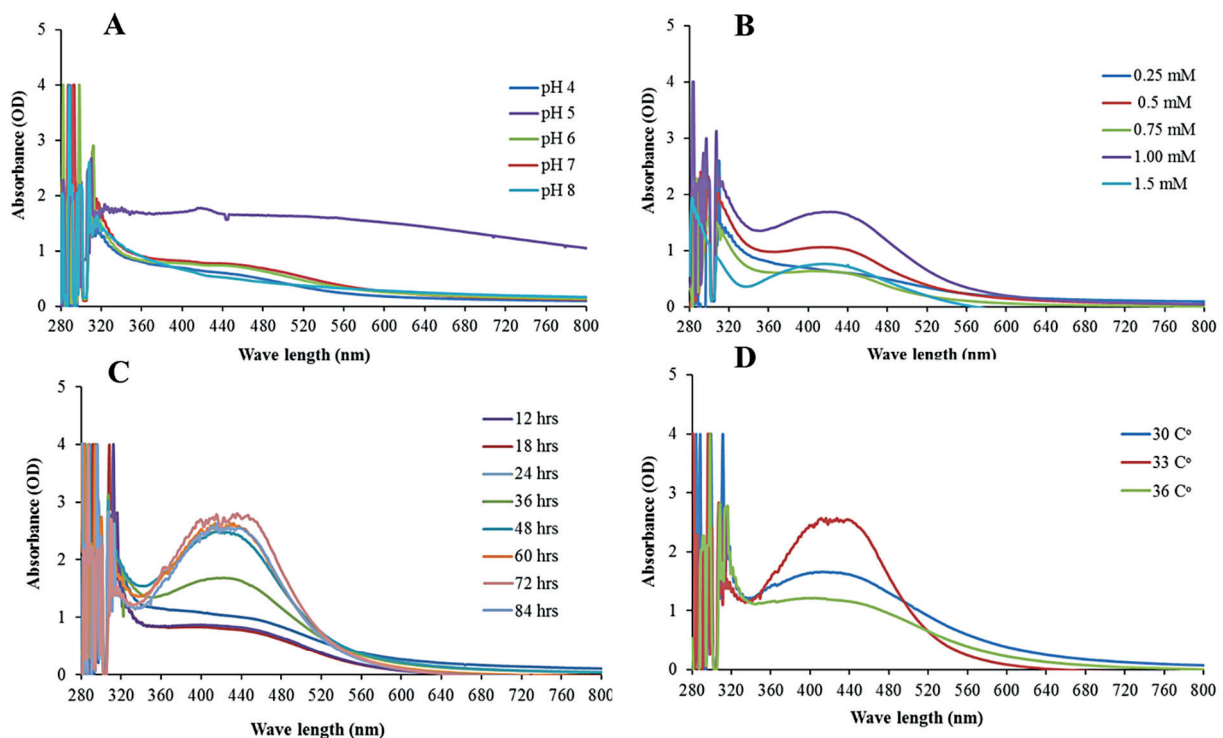


**Figure 3.** (A) Effect of pH on the bio-reduction of AgNO<sub>3</sub>; (B) Effects of silver nitrate concentration on its bio-reduction; (C) Effects of the reaction time on the bio-reduction of AgNO<sub>3</sub>; (D) Effects of incubation temperature on the bio-reduction of AgNO<sub>3</sub>

of temperature on vital specific enzymes in the filtrate generated from *R. stolonifer* MR11 biomass. The results, however, revealed that the optimal temperatures for cell growth and silver accumulation differ. AgNPs were established at lower temperatures, but not to the extent that the absorbance scan indicated. Increasing the reaction temperature may improve both the rate of  $\text{AgNO}_3$  adsorption and the coat-phase viscosity (Gurunathan et al., 2009). As a result, the possibility of AgNPs accumulation is reduced, and thus smaller particles are produced (Alfarayeh et al., 2021a; Song and Kim, 2009).

### ATR-IR spectrum analysis

The ATR-FTIR spectrum (Figure 4) disclosed definite peaks at 1011, 1375, 1437, 1516, 1623, 2401  $\text{cm}^{-1}$ , and a quite floppy peak at ca. 3228  $\text{cm}^{-1}$ . The wide peak between 3228  $\text{cm}^{-1}$  and 2827  $\text{cm}^{-1}$ , coincides with the vibrational resonances of hydrogen-containing bonds such as C-H, O-H, and N-H. The symmetric and asymmetric stretching of the COO- group is indicated by the high absorption intensity values peaks at 1623, 1516, and 1081  $\text{cm}^{-1}$ . The spectrum simply proves peaks at 1375  $\text{cm}^{-1}$  of the stretching frequency of the protein's amino and amino-methyl stretching groups.

### XRD analysis

The XRD spectrum ( $2\theta = 0^\circ$  to  $80^\circ$ ) reveals four significant and strong Bragg reflections at  $2\theta = 37.72^\circ$ ,  $44.08^\circ$ ,  $64.36^\circ$ , and  $77.16^\circ$ . This XRD pattern indicates the formation of multi-crystalline silver nanoparticles (Figure 5). These strong Bragg reflections correlate to the crystallographic planes (111), (200), (220), and (331), respectively, of face-centered cubic (FCC) silver crystals. The size of the nanoparticles is estimated by using classical Scherrer's formula [lit] with a geometric factor of 0.94 over the (111) reflection. The sample crystallite diameters are found to be approximately 6.997 nm.

### Particle size, zeta potential, and morphology

The resulting AgNPs had an average diameter of 307.3 nm and a PDI value of 0.704 (Figure 6A). As a result, the PDI (DLS) was greater than 0.2, indicating that the apportionment was polydisperse (Cascio et al., 2015; Soliman et al., 2021). The PDI value was nearly greater than 0.7, indicating that the specimen has a very broad distribution of particle size and is thus unlikely to be useful for processing using the DLS (technique of dynamic light scattering) (Danaei et al., 2018). The zeta potential was -16.6 mV (Figure 6B). Because particles with an appropriate charge are electrostatically constant and thus resist self-assembly, they

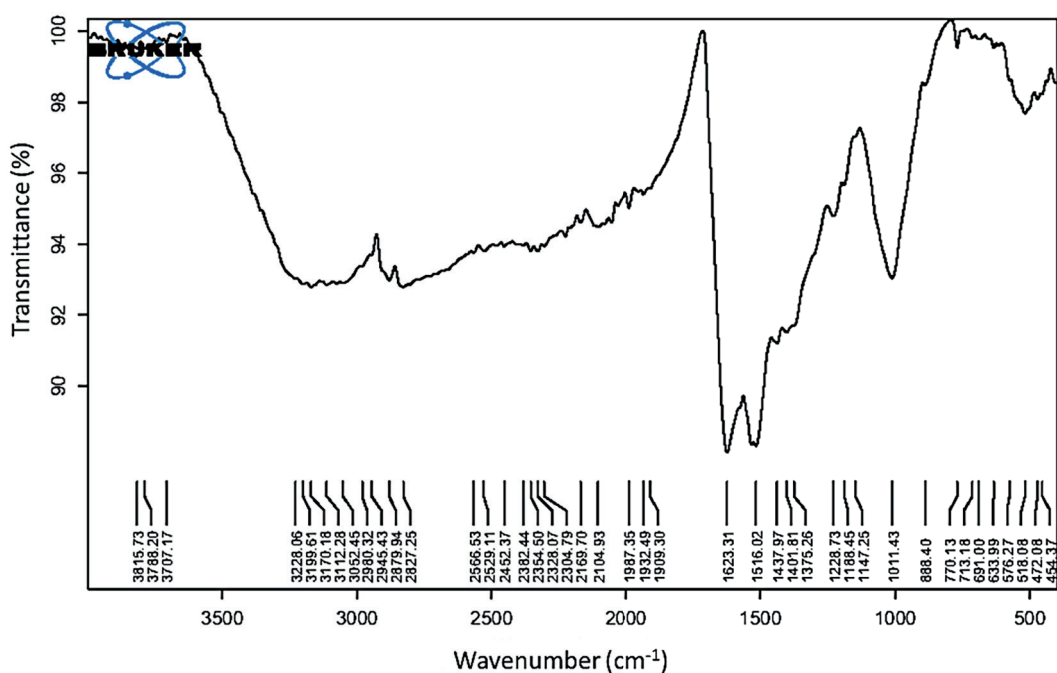


Figure 4. ATR-IR analysis of biologically synthesized silver nanoparticles

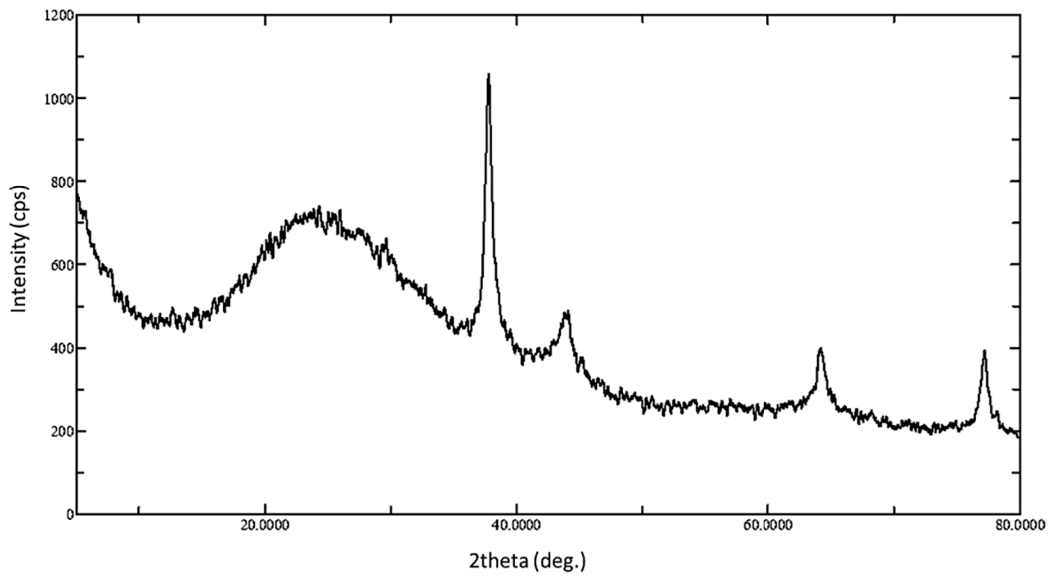


Figure 5. XRD analysis of biologically synthesized silver nanoparticles

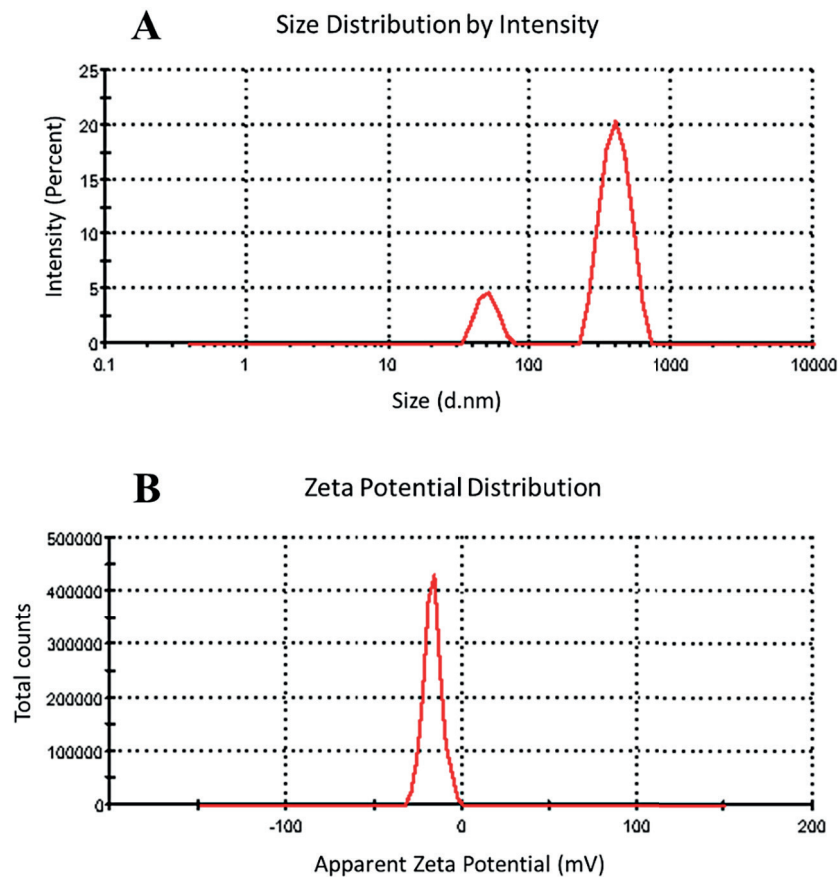
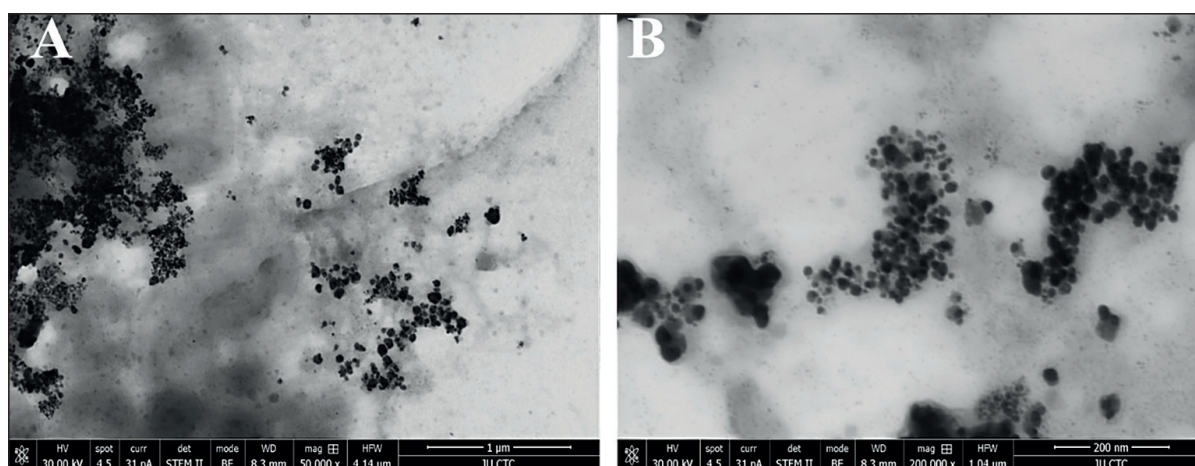


Figure 6. (A) The size distribution by the intensity of AgNPs nanoparticles. The average size of the nanoparticles is about 307.3 nm; (B) Zeta potential distribution of silver nanoparticles. AgNPs zeta potential shows -16.6 mV

have Z values of this size. The Z-Average is the result of a cumulative analysis that determines the hydrodynamic size of the measured auto-conduction function based on the assumption that the sample is monodisperse. Figures 6A

and B illustrate the probability that more than one volume exists in the sample, so quoting the mean Z in this manner may be inappropriate. The density distribution in our sample illustrates the relative amount of scattering from



**Figure 7.** TEM Image of biosynthesized silver nanoparticles. Magnification (A) 50,000x, (B) 200,000x

groups of various sizes. Due to the fact that light scattering is proportional to particle size, a small amount of a larger component may dominate the gesture. The Number distribution report utilizes the optical properties of the sample to present the relative number based on the size distribution from the data of density distribution (Cascio et al., 2015). The AgNPs were found to be regular and spherical using transmission electron microscopy (TEM) observations (Figures 7A and B). TEM micrographs revealed that the AgNPs were smaller than those observed by the DLS examination due to particle shrinkage caused by the drying process. AgNPs had an average size of less than 35 nm.

## CONCLUSIONS

The potential of *R. stolonifer* MR11 to effectively reduce silver nitrate to AgNPs was demonstrated. The establishment of AgNPs was revealed by a color change of the silver nitrate solution and UV-Vis spectra. The growth conditions, conditions under which the biomass filtrate was obtained, and bio-reduction reaction conditions that control the biosynthesis of AgNPs are all critical. Thus, the AgNPs biosynthesis results highlighted the importance of the studied parameters at each level of the process. It is proposed that any of the parameters in one of the three-step involved in the biosynthesis of AgNPs could be optimized. Therefore, to obtain higher production of nanoparticles all the parameters starting from the growth of the fungi to the last step of the biosynthesis of AgNPs should be evaluated.

## Acknowledgments

The authors would like to thank the Deanship of Scientific Research at Mutah University/Jordan for supporting this research with grant proposals 315/2020 and 347/2020.

## REFERENCES

- Alfarrayeh I., Fekete C., Gazdag Z., Papp G. 2021. Propolis ethanolic extract has double-face in vitro effect on the planktonic growth and biofilm formation of some commercial probiotics. *Saudi Journal of Biological Sciences*, 28(1), 1033–1039.
- Alfarrayeh I., Pollák E., Czéh Á., Vida A., Das S., Papp G. 2021. Antifungal and Anti-Biofilm Effects of Caffeic Acid Phenethyl Ester on Different Candida Species. *Antibiotics*, 10(11), 1359–1374.
- Balakumaran M.D., Ramachandran R., Kalaichelvan P.T. 2015. Exploitation of endophytic fungus, *Guignardia mangiferae* for extracellular synthesis of silver nanoparticles and their in vitro biological activities. *Microbiological research*, 178, 9–17.
- Basavaraja S., Balaji S.D., Lagashetty A., Rajasab A.H., Venkataraman A. 2008. Extracellular biosynthesis of silver nanoparticles using the fungus *Fusarium semitectum*. *Materials Research Bulletin*, 43(5), 1164–1170.
- Bhainsa K.C., D'souza S.F. 2006. Extracellular biosynthesis of silver nanoparticles using the fungus *Aspergillus fumigatus*. *Colloids and surfaces B: Biointerfaces*, 47(2), 160–164.
- Calderón-Jiménez B., Johnson M.E., Montoro Bustos A.R., Murphy K.E., Winchester M.R., Vega Baudrit J.R. 2017. Silver nanoparticles: Technological advances, societal impacts, and metrological challenges. *Frontiers in chemistry*, 5, 6.

7. Cascio C., Geiss O., Franchini F., Ojea-Jimenez I., Rossi F., Gilliland D., Calzolari L. 2015. Detection, quantification and derivation of number size distribution of silver nanoparticles in antimicrobial consumer products. *Journal of Analytical Atomic Spectrometry*, 30(6), 1255–1265.
8. Colvin V.L., Schlamp M.C., Alivisatos A.P. 1994. Light-emitting diodes made from cadmium selenide nanocrystals and a semiconducting polymer. *Nature*, 370(6488), 354–357.
9. Dallas P., Sharma V.K., Zboril R. 2011. Silver polymeric nanocomposites as advanced antimicrobial agents: classification, synthetic paths, applications, and perspectives. *Advances in Colloid and Interface Science*, 166(1–2), 119–135.
10. Danaei M., Dehghankhold M., Ataei S., Hasanazadeh Davarani F., Javanmard R., Dokhani A., Khorasani S., Mozafari M.R. 2018. Impact of particle size and polydispersity index on the clinical applications of lipidic nanocarrier systems. *Pharmaceutics*, 10(2), 57.
11. Durán N., Marcato P.D., Alves O.L., De Souza G.I.H., Esposito E. 2005. Mechanistic aspects of biosynthesis of silver nanoparticles by several *Fusarium oxysporum* strains. *Journal of Nanobiotechnology*, 3(1), 1–7.
12. Elamawi R.M., Al-Harbi R.E., Hendi A.A. 2018. Biosynthesis and characterization of silver nanoparticles using *Trichoderma longibrachiatum* and their effect on phytopathogenic fungi. *Egyptian Journal of Biological Pest Control*, 28(1), 1–11.
13. Fabrega J., Luoma S.N., Tyler C.R., Galloway T.S., Lead J.R. 2011. Silver nanoparticles: behaviour and effects in the aquatic environment. *Environment International*, 37(2), 517–531.
14. García-Barrasa J., López-de-Luzuriaga J.M., Monge M. 2011. Silver nanoparticles: synthesis through chemical methods in solution and biomedical applications. *Central European Journal of Chemistry*, 9(1), 7–19.
15. Gentile A., Ruffino F., Grimaldi M.G. 2016. Complex-morphology metal-based nanostructures: Fabrication, characterization, and applications. *Nanomaterials*, 6(6).
16. Guilger-Casagrande M., de Lima R. 2019. Synthesis of silver nanoparticles mediated by fungi: a review. *Frontiers in Bioengineering and Biotechnology*, 7, 287.
17. Gurunathan S., Kalishwaralal K., Vaidyanathan R., Venkataraman D., Pandian S.R.K., Muniyandi J., Hariharan N., Eom S.H. 2009. Biosynthesis, purification and characterization of silver nanoparticles using *Escherichia coli*. *Colloids and Surfaces B: Biointerfaces*, 74(1), 328–335.
18. Ingole A.R., Thakare S.R., Khati N.T., Wankhade A.V., Burghate D.K. 2010. Green synthesis of selenium nanoparticles under ambient condition. *Chalcogenide Lett*, 7(7), 485–489.
19. Jaidev L.R., Narasimha G. 2010. Fungal mediated biosynthesis of silver nanoparticles, characterization and antimicrobial activity. *Colloids and Surfaces B: Biointerfaces*, 81(2), 430–433.
20. Kalimuthu K., Babu R.S., Venkataraman D., Bilal M., Gurunathan S. 2008. Biosynthesis of silver nanocrystals by *Bacillus licheniformis*. *Colloids and Surfaces B: Biointerfaces*, 65(1), 150–153.
21. Klaus T., Joerger R., Olsson E., Granqvist C.-G. 1999. Silver-based crystalline nanoparticles, microbially fabricated. *Proceedings of the National Academy of Sciences*, 96(24), 13611–13614.
22. Lee S.H., Jun B.-H. 2019. Silver nanoparticles: synthesis and application for nanomedicine. *International Journal of Molecular Sciences*, 20(4), 865.
23. Mukherjee P., Senapati S., Mandal D., Ahmad A., Khan M.I., Kumar R., Sastry M. 2002. Extracellular synthesis of gold nanoparticles by the fungus *Fusarium oxysporum*. *ChemBioChem*, 3(5), 461–463.
24. Padalia H., Moteriya P., Chanda S. 2015. Green synthesis of silver nanoparticles from marigold flower and its synergistic antimicrobial potential. *Arabian Journal of Chemistry*, 8(5), 732–741.
25. Qian Y., Yu H., He D., Yang H., Wang W., Wan X., Wang L. 2013. Biosynthesis of silver nanoparticles by the endophytic fungus *Epicoccum nigrum* and their activity against pathogenic fungi. *Bioprocess and Biosystems Engineering*, 36(11), 1613–1619.
26. Sanghi R., Verma P. 2009. Biomimetic synthesis and characterisation of protein capped silver nanoparticles. *Bioresource Technology*, 100(1), 501–504.
27. Satalkar P., Elger B.S., Shaw D.M. 2016. Defining nano, nanotechnology and nanomedicine: why should it matter? *Science and Engineering Ethics*, 22(5), 1255–1276.
28. Sergeev G.B., Shabatina T.I. 2008. Cryochemistry of nanometals. *Colloids and Surfaces A: Physicochemical and engineering aspects*, 313, 18–22.
29. Singh D., Rathod V., Ninganagouda S., Hiremath J., Singh A.K., Mathew J. 2014. Optimization and characterization of silver nanoparticle by endophytic fungi *Penicillium* sp. isolated from *Curcuma longa* (turmeric) and application studies against MDR *E. coli* and *S. aureus*. *Bioinorganic Chemistry and Applications*, 2014.
30. Singh R., Wagh P., Wadhvani S., Gaidhani S., Kumbhar A., Bellare J., Chopade B.A. 2013. Synthesis, optimization, and characterization of silver nanoparticles from *Acinetobacter calcoaceticus* and their enhanced antibacterial activity when combined with antibiotics. *International Journal of Nanomedicine*, 8, 4277.

31. Soliman A.M., Abdel-Latif W., Shehata I.H., Fouda A., Abdo A.M., Ahmed Y.M. 2021. Green approach to overcome the resistance pattern of *Candida* spp. using biosynthesized silver nanoparticles fabricated by *Penicillium chrysogenum* F9. *Biological Trace Element Research*, 199(2), 800–811.
32. Song J.Y., Kim B.S. 2009. Rapid biological synthesis of silver nanoparticles using plant leaf extracts. *Bioprocess and Biosystems Engineering*, 32(1), 79–84.
33. Williams D. 2008. The relationship between biomaterials and nanotechnology. *Biomaterials*, 29(12), 1737–1738.
34. Xu Z.P., Zeng Q.H., Lu G.Q., Yu A.B. 2006. Inorganic nanoparticles as carriers for efficient cellular delivery. *Chemical Engineering Science*, 61(3), 1027–1040.